NASA TECHNICAL NOTE

NASA TN D-8342

NASA TN D-8342

PERFORMANCE AND EMISSION CHARACTERISTICS OF SWIRL-CAN COMBUSTORS TO A NEAR-STOICHIOMETRIC FUEL-AIR RATIO

Larry A. Diehl and Arthur M. Trout

Lewis Research Center
Cleveland, Ohio 44135

NATIONAL AERONAUTICS AND SPACE ADMINISTRATION • WASHINGTON, D. C. • NOVEMBER 1976

1. Report No.	2. Government Accession No.	3. Recipient's Catalog No.
NASA TN D-8342		

4. Title and Subtitle	5. Report Date
PERFORMANCE AND EMISSION CHARACTERISTICS OF SWIRL-CAN COMBUSTORS TO NEAR-STOICHIOMETRIC FUEL-AIR RATIO	November 1976
	6. Performing Organization Code
7. Author(s)	8. Performing Organization Report No.
Larry A. Diehl and Arthur M. Trout	E-8718
	10. Work Unit No.
9. Performing Organization Name and Address	505-03
Lewis Research Center National Aeronautics and Space Administration Cleveland, Ohio 44135	11. Contract or Grant No.
	13. Type of Report and Period Covered
12. Sponsoring Agency Name and Address	Technical Note
National Aeronautics and Space Administration Washington, D.C. 20546	14. Sponsoring Agency Code

15. Supplementary Notes

16. Abstract

Emissions and performance characteristics were determined for two full-annular swirl-can combustors operated to near-stoichiometric fuel-air ratio. Test condition variations were as follows: combustor inlet-air temperatures, 589, 756, 839, and 894 K; reference velocities, 24 to 37 meters per second; inlet pressure, 62 newtons per square centimeter; and fuel-air ratios, 0.015 to 0.065. The combustor average exit temperature and combustor efficiency were calculated from the combustor exhaust gas composition. For fuel-air ratios greater than 0.04 the combustion efficiency decreased with increasing fuel-air ratios in a near-linear manner. Increasing the combustor inlet-air temperature tended to offset this decrease. Maximum oxides of nitrogen emission indices occurred at intermediate fuel-air ratios and were dependent on combustor design. Carbon monoxide levels were extremely high and were the primary cause of poor combustion efficiency at the higher fuel-air ratios. Unburned hydrocarbons were low for all test conditions. For high fuel-air ratios SAE smoke numbers greater than 25 were produced, except at the highest inlet-air temperatures.

17. Key Words (Suggested by Author(s))	18. Distribution Statement
Air pollution; Combustion; Combustion chambers; Combustion efficiency; Combustion products; Exhaust gases; Hydrocarbon combustion; Gas turbine engines	Unclassified - unlimited STAR Category 07

19. Security Classif. (of this report)	20. Security Classif. (of this page)	21. No. of Pages	22. Price*
Unclassified	Unclassified	40	$4.00

* For sale by the National Technical Information Service, Springfield, Virginia 22161

PERFORMANCE AND EMISSION CHARACTERISTICS OF SWIRL-CAN COMBUSTORS TO A NEAR-STOICHIOMETRIC FUEL-AIR RATIO

by Larry A. Diehl and Arthur M. Trout

Lewis Research Center

SUMMARY

Emissions and performance characteristics were determined for two full-annular swirl-can combustors operated to near-stoichiometric fuel-air ratio. The measured exhaust gas composition included oxides of nitrogen, carbon monoxide, carbon dioxide, oxygen, unburned hydrocarbons, and smoke. Test condition variations were as follows: combustor inlet-air temperatures, 589, 756, 839, and 894 K; reference velocities, 24 to 37 meters per second; inlet pressure, 62 newtons per square centimeter; and fuel-air ratios, 0.015 to 0.065.

The combustor average exit temperature and combustor efficiency were calculated from the combustor exhaust gas composition. For fuel-air ratios greater than 0.040, combustion efficiency decreased with increasing fuel-air ratios in a near-linear manner. Increasing the combustor inlet-air temperature tended to offset this decrease. Increasing the inlet-air temperature from 589 to 894 K at a fuel-air ratio of 0.064 increased the combustion efficiency from 91 to 95 percent.

The maximum oxides of nitrogen emission indices occurred at intermediate fuel-air ratios. The value of the fuel-air ratio for maximum NO_x production was dependent on the combustor design and, in particular, the amount of air admitted through the swirl-can module.

Carbon monoxide emissions increased rapidly for fuel-air ratios greater than 0.040 and reached levels of 450 to 650 grams per kilogram depending on the combustor inlet-air temperature. This constituent was the primary cause of poor combustion efficiency at the higher fuel-air ratios.

Unburned hydrocarbon emissions were 10 grams per kilogram or less at an inlet-air temperature of 589 K and 4 grams per kilogram or less at the higher inlet-air temperatures.

For fuel-air ratios below 0.035 the smoke emissions were negligible. An SAE smoke number of 25 was exceeded at the following combinations of fuel-air ratio and inlet-air temperatures: 0.047 at 589 K, 0.055 at 756 K, and 0.059 at 839 K. A smoke number of 25 was not exceeded at any fuel-air ratio investigated at the 894 K inlet temperature.

INTRODUCTION

An experimental test program was conducted to determine the emissions and performance characteristics of two full-annular three-row swirl-can combustors operated to near-stoichiometric fuel-air ratios. Measured emissions included oxides of nitrogen, carbon monoxide, unburned hydrocarbons, and smoke.

Swirl-can combustors have been investigated for many years at the Lewis Research Center. Initial tests of a swirl-can combustor operated to near-stoichiometric exit temperatures are reported in reference 1. More recent studies (refs. 2 and 3) have included pollutant emissions measurements at stoichiometric conditions. In these previous studies, stoichimetric operation was achieved at a combustor inlet-air temperature of 589 K only. The present study extended the operating region of these combustors to the higher inlet-air temperatures and evaluated the effect of recent refinements in the swirl-can module design. In addition, the previous work relied on a choked nozzle as the primary means of determining combustion efficiency. Since in the combustor test stand the choked nozzle effectively decouples the downstream exhaust valve, independent control of combustor temperature, pressure, and airflow is not possible. For this study the choked nozzle was eliminated and a gas analysis technique was used to determine the combustion efficiency. While combustion efficiency can be inferred from the emission measurement of the previous studies, the results are somewhat restricted as samples were obtained at a single circumferential location. Since the time of the last reported stoichiometric tests, a considerable effort has resulted in the successful development of a traversing emissions sampling system suitable for the high combustor exit temperatures involved. The emissions sampling system samples both radially and circumferentially virtually all of the combustor exit annulus area.

One of the prime applications for swirl-can combustors has always been deemed to be in engines requiring very high turbine-inlet temperatures. There are several design features which make them suitable for high temperature applications:

(1) The large number of modules distributes combustion uniformly across the annulus. All of the combustor airflow, exclusive of liner coolant flow, passes through the array.

(2) The individual modules in the array perform several functions. Each module achieves some degree of premixing fuel and air, swirls the mixture, stabilizes combustion in its wake, and provides large interfacial mixing areas between the bypass air through the array and the hot gases in the module wake.

(3) Only small amounts of coolant flow are required because of the short combustor length and the combustor liner design. The liner follows a contour such that the major portion of it is removed from the hot gas streamlines. For high temperature-rise applications, the requirement of small liner flows is necessary to minimize the tendency towards a peaked radial temperature profile at the combustor exit. Any air used for

liner cooling, and not available for combustion, lowers the maximum achievable combustor exit temperature.

The swirl-can combustor has also achieved considerable attention as a combustor design suitable for reducing oxides of nitrogen emissions. It is interesting to note that the features cited previously as being desirable for high temperature-rise operation offer advantages for reducing oxides of nitrogen. These advantages include the following:

(1) Short combustor lengths with accompanying short recirculation zones are realized for burning and mixing. Thus dwell time is reduced.

(2) Quick mixing of burning gases and diluent air occurs inasmuch as swirl-can combustors pass nearly all of the airflow through the primary combustion zone, and large interfacial mixing areas exist between combustion gases and airflow around the swirl-cans.

(3) A more uniform mixture of fuel and air is produced by the large number of fuel entry points, thereby reducing localized intense burning.

Two versions of a 120-module swirl-can combustor were tested to determine emissions of oxides of nitrogen, carbon monoxide, unburned hydrocarbons, and smoke for combustor average fuel-air ratios approaching stoichiometric. Combustor average-exit temperature and combustion efficiency were calculated from the combustor emissions as determined from a total traverse survey at the combustor exit. For average-exit temperatures to 1700 K thermocouples were available for direct temperature measurement. Test conditions included the following: combustor inlet air temperatures, 589, 756, 839, 894 K; reference velocity, 24 to 37 meters per second; inlet pressure, 62 newtons per square centimeter; and fuel-air ratio, 0.015 to 0.065. All tests were conducted using ASTM Jet-A fuel.

APPARATUS AND PROCEDURE

Test Facility

Testing was conducted in a closed-duct test facility at the Lewis Research Center. A schematic of this facility is shown in figure 1. A detailed description of the facility and instrumentation are contained in reference 4. All fluid flow rates and pressures are controlled remotely.

Combustor Design

The test combustor, shown in figures 2 and 3, is an annular design - 51.4 centime-

ters long from the diffuser inlet to the combustor exit plane and 106.2 centimeters in outer diameter. The combustor array consists of 120 modules positioned on three circumferential rows. There are 48 modules on the outer row, 40 modules in the center row, and 32 modules in the inner row. The inlet diffuser passage for both configurations was 12.3 centimeters long and had an exit area to inlet area ratio of 1.45. The diffuser was followed by a sudden expansion region in which the ratio of the annular flow area at the inlet plane of the swirl-cans to the diffuser-exit area was 2.42. Combustor reference area was 0.549 square meter. The only airflow introduced downstream of the array is liner cooling air which accounted for 9 to 12 percent of the total airflow.

Module Design

Two module designs were used for these tests and are shown in figure 4. Each module consisted of a carburetor, a cone swirler, and a flame stabilizer. The conical fuel swirlers used in this study are an evolutionary development over the flat bladed swirlers used in references 1 to 3. The newer design offers improved combustion efficiency at low power conditions and improved durability at high power conditions. However, compared to the previous design these swirlers produce higher oxides of nitrogen emissions. The two designs shown in figure 4 differed in method and location of fuel entry, swirler design, and flame stabilizer geometry. For combustor module 1 the fuel was injected from a circumferential slot at the end of the fuel tube so that it impacted the downstream surface of the swirler between the radial inflow blades (fig. 4). This model employed two types of flame stabilizers which produced a design blockage of 61 percent. For combustor model 2 the fuel was injected so that it impacted the apex of the axial flow cone swirler. A uniform flame stabilizer design provided a design blockage of 67 percent. The effective open area of the swirlers was determined by a single element airflow test rig and was 1.85 square centimeters for model 1 and 3.45 square centimeters for model 2. A sector view of each of these combustors is presented in figure 5.

Exhaust Gas Temperatures and Pressures

For average exhaust gas temperatures to 1700 K, the combustor exit total temperatures and pressures were measured with three equally spaced five-point thermocouple and total pressure rakes driven by a drum assembly which traversed circumferentially in the exit plane. The drum assembly moved in 3^{o} increments and required approximately 7 minutes for a complete survey. Five hundred eighty-five individual exit temperatures were obtained in each traverse. The temperatures were used to check for an

acceptable radial profile and for temperature nonuniformities. For tests performed at average exhaust gas temperatures greater than 1700 K the temperature and pressure probes were removed and three five-point fixed total pressure probes were installed approximately 10 centimeters downstream of the combustor exit. Average exhaust gas temperatures were calculated from the gaseous emissions products. Details concerning this calculation may be found in the appendix.

Exhaust Emissions

Concentrations of nitric oxide, total oxides of nitrogen, carbon monoxide, unburned hydrocarbons, oxygen, and carbon dioxide were obtained with an online sampling system. The sample was drawn at the combustor exit plane by means of three commonly manifolded water-cooled traversing probes. Each probe had five sample locations located on centers of equal area. These probes were positioned on the previously mentioned traversing assembly midway between the temperature and pressure probe locations. A photograph of the traverse assembly is presented in figure 6.

Gas sample system. - A schematic of the gas analysis system is shown in figure 7. The samples collected by the three sample probes were commonly manifolded to one sample line. The line was steam heated to 420 K. Sample line pressure was maintained at 17 newtons per square centimeter in order to supply sufficient pressure to operate the instruments. Sufficient sample was vented at the instruments to minimize line residence time (about 2 sec).

The exhaust gas analysis system was a packaged unit consisting of five commercially available instruments along with associated peripheral equipment necessary for sample conditioning and instrument calibration. In addition to visual readout, electrical inputs were provided to an IBM 360/67 computer for an online analysis and evaluation of the data.

The hydrocarbon content of the exhaust gas was determined by a Beckman Instruments model 402 hydrocarbon analyzer. This instrument is of the flame ionization detector type.

The oxygen analyzer is a Beckman Instruments model 778 and is a polarographic type. The combustor inlet-air humidity was measured with an EG&G model 880 dew point hygrometer.

The concentration of the oxides of nitrogen was determined by a Thermo Electron Corporation model 10A chemiluminescent analyzer. The instrument includes a thermal reactor to reduce NO_2 to NO and was operated at 973 K.

Both carbon monoxide (CO) and carbon dioxide (CO_2) analyzers were of the nondispersive infrared (NDIR) type (Beckman Instruments model 315B). The CO analyzer had four ranges: 0 to 100 ppm, 0 to 1000 ppm, 0 to 1 percent, and 0 to 10 percent. These

ranges of sensitivity were obtained by using stacked cells that were 0.64 and 34 centimeters in length. The CO_2 analyzer had two ranges: 0 to 5 percent and 0 to 15 percent with a sample cell length of 0.32 centimeter.

Analytical procedure. - All analyzers were checked for zero and span prior to the test. Solenoid switching within the console allowed rapid selection of zero, span, or sample modes. Therefore, it was possible to perform frequent checks to ensure calibration accuracy without disrupting testing.

Where appropriate, the measured quantities were corrected for water vapor removed. The correction included both inlet-air humidity and water vapor from combustion. The equations used are given in the appendix.

The emission levels of all the constituents were converted to an emission index (EI) parameter. The EI for any constituent X is given by

$$EI_X = \frac{M_x}{M_E} \frac{1+f}{f} [X] 10^{-3}$$

where

EI_X emission index in g of X/kg of fuel burned

M_x molecular weight of X

M_E average molecular weight of exhaust gas

f metered fuel-air ratio (g of fuel/g of air)

[X] measured concentration of X in ppm of exhaust gas

Sample Validity

For each test point a fuel-air ratio was calculated from the gaseous emissions according to the relation shown in the appendix. A comparison of gas sampling to metered fuel-air ratios for all data is shown in figure 8. Since nominally 10 percent of the total combustor air flow was used for liner cooling and since the gas sample probes did not give total coverage of the liner cooling air, it is reasonable to expect that emission based fuel-air ratios obtained at the combustor exit should be greater than a fuel-air ratio based on metered fuel and airflow. The computed mean value is 1.027 with a standard deviation of 0.030. Slightly more than 93 percent of the data are within ±5 percent of the mean value.

Smoke Number Measurement

The smoke sampling procedure as recommended in reference 5 was followed as closely as possible. The samples were drawn at approximately 8 centimeters downstream of the combustor exit plane illustrated in figure 2 from one circumferential location at three radial positions through a water-cooled stainless-steel probe. The sample was transported to the filtering material (Whatman No. 4 filter paper) through approximately 4.5 meters of stainless-steel line.

The sample rate through the filter was 2.36×10^{-4} cubic meter per second. The filter was placed on a black background tile to measure comparative reflectance using a Welch Densichron and Reflection unit (0.3832 μm). A Welch Gray Scale (cat. no. 3827 T) was used as a calibration reference.

Test Conditions

The nominal combustor operating conditions are listed in table I. For all tests the combustor airflow was 50 kilograms per second and combustor pressure was 62 newtons per square centimeter. At a given combustor inlet-air temperature, data were obtained with an increasing combustor fuel-air ratio up to the maximum recorded. As a check on consistency, data were also obtained with decreasing fuel-air ratio at points intermediate to these previously obtained.

Calculations

Combustor exit temperature and efficiency from gas analysis. - Exit temperature was determined from the numerically averaged emissions obtained from the combustor traverse according to the procedure given in the appendix. The efficiency as used in this report is defined as the ratio of measured temperature rise across the combustor to the theoretical temperature rise.

Radial profile factors. - Profile factors were calculated only for those test conditions where thermocouple traverse measurements were made. The radial profile of exit temperature was established from the circumferential average of the temperature at each radial position and was plotted as a deviation from the average exit temperature as a function of radial position. To detect temperature nonuniformities which may not be evident in the average radial profile, three temperature profile quality factors were calculated: exit temperature pattern factor $\overline{\delta}$, stator factor δ_{stator}, and rotor factor δ_{rotor}.

The exit temperature pattern factor $\overline{\delta}$ was used to reflect the magnitude of nonuniformity caused by the maximum local temperature. This factor was defined as

$$\overline{\delta} = \frac{T_{max} - T_{av}}{\Delta T_{av}}$$

where T_{max} is the maximum individual exit temperature, T_{av} the mass-weighted average exit temperature determined from the procedure of reference 6 and using the 585 individual exit temperatures, and ΔT_{av} the temperature difference between the mass-weighted average exit temperature and the average inlet temperature. To measure the magnitude of temperature nonuniformity which affects turbine stator vanes, a stator factor δ_{stator} was defined as

$$\delta_{stator} = \frac{\left(T_{r,max} - T_{r,design}\right)_{max}}{\Delta T_{av}}$$

To measure the magnitude of temperature nonuniformity which affects turbine rotor blades, a rotor factor δ_{rotor} was defined as

$$\delta_{rotor} = \frac{\left(T_{r,av} - T_{r,design}\right)_{max}}{\Delta T_{av}}$$

In these equations $T_{r,max}$ is an individual maximum radial temperature and $T_{r,av}$ is an average radial temperature which, when compared with the corresponding design radial average temperature $T_{r,design}$, yield the maximum positive temperature difference and the largest radial profile factor.

Reference velocity and Mach number. - Reference conditions were based on the total airflow, the total and static pressure and total temperature at the diffuser inlet, and the reference area of 0.549 square meter. The reference area was the maximum cross-sectional area of the combustor.

Total-pressure loss. - Combustor total-pressure loss was calculated as the difference between 40 averaged total pressures measured upstream of the diffuser inlet and 585 averaged total pressures measured at the combustor exit divided by the averaged upstream total pressure. Therefore, the combustor total-pressure loss includes the diffuser loss. For the test conditions where the traversing pressure and thermocouple probes were removed, only the 15 averaged total pressures obtained from the three fixed rakes were used.

Diffuser inlet Mach number. - Diffuser inlet total and static pressure and total temperature were used for calculating the inlet Mach number.

RESULTS AND DISCUSSION

Performance and emissions characteristics of the combustors are presented in tables II and III. Significant characteristics of the combustors are discussed in this section.

For Jet-A fuel the stoichiometric fuel-air ratio is 0.068. The maximum test fuel-air ratio was about 0.064. The fuel-air ratio was deliberately maintained slightly below the stoichiometric value in an attempt to minimize burning with the liner cooling air.

Total-Pressure Loss

The isothermal pressure loss for both combustors is shown in figure 9. The pressure loss for the combustors shown here is comparable to that of combustors currently in use. The maximum recorded pressure loss with burning, which occurred with model 2 at a fuel-air ratio of 0.0637 at the 894 K inlet-air temperature test condition, was 7.61 percent.

Heat Release Rate

The maximum heat release rate, which occurred at the 0.064 test fuel-air ratio, was 6.6×10^{11} joules per cubic meter per hour per newton per square meter ($J/m^3/hr/(N/m^2)$) (18×10^6 $Btu/ft^3/hr/atm$). At a more conventional fuel-air ratio of 0.023 the value would be 2.4×10^{11} $J/m^3/hr/(N/m^2)$ (6.4×10^6 $Btu/ft^3/hr/atm$). Values of from 1.9 to 3.0×10^{11} $J/m^3/hr/(N/m^2)$ (5 to 8×10^6 $Btu/ft^3/hr/atm$) are typical of current combustor technology.

Exit Temperature Distribution

A summary of the combustor exit temperature profile factors is given in table II. Combustor model 1 had undergone some preliminary testing prior to these tests. Combustor model 2 design was based on the results of similar models but had not been previously tested and therefore exhibited higher pattern factor than model 1. It is recognized that high pattern factor is undesirable and with regard to emissions is a

contributor to high oxides of nitrogen due to local high temperature regions. Nevertheless, it was felt that in the demonstration of the high temperature-rise capabilities of these combustors, the refinement of the temperature profile factors to lower levels was beyond the scope of the investigation.

A typical average radial exit temperature profile for each of the combustor models is shown plotted against an arbitrary desired profile in figure 10. The radial profiles were in general cold at the tip. The maximum individual (local) temperatures at each radial position are also shown in this figure. For combustor model 1 the maximum average radial profile temperature difference from the design profile was 26 K, which corresponds to a rotor factor of 0.038, and the maximum individual (local) temperature difference from the desired profile was 117 K, which corresponds to a stator factor of 0.20. For combustor model 2 the maximum average radial profile temperature difference was 53 K, which corresponds to a rotor factor of 0.092, and the maximum individual (local) temperature difference was 223 K, which corresponds to a stator factor of 0.39.

Gaseous Exhaust Emissions

A summary of the combustor exhaust gas emissions is presented in table III. The emissions are presented both in terms of an emission index (g of pollutant/kg of fuel) and parts per million by volume.

Unburned hydrocarbons. - The emission index for unburned hydrocarbons is shown in figure 11. With the exception of the 589 K inlet-air temperature the hydrocarbon levels were low even at the highest fuel-air ratios. In all cases the emission index values were 10 grams per kilogram of fuel or less. Minimum emissions were recorded in the 0.03 to 0.04 fuel-air ratio range. For model 2 at the 589 K inlet-air temperature some hydrocarbons are present even in the fuel-air ratio range of 0.03 to 0.04. It will be shown in a later section of this report that this combustor had a significant loss in combustion efficiency at this condition. As the overall fuel-air ratio is increased to near stoichiometric, a loss in combustion efficiency will occur due to overly fuel-rich conditions which will eventually form in the module wakes. The swirler open area for model 2 was intentionally made large to delay the onset of this loss in combustion efficiency. The extent to which the swirler open area was increased resulted in some loss of combustion efficiency at the lower inlet-air temperatures and fuel-air ratios. Therefore, the previously mentioned design advantage of the cone fuel swirler of having high idle efficiency was deliberately sacrificed in an attempt to extend its operating region to the higher fuel-air ratios. The excellent core swirler durability characteristics would remain however. Note that as a result of this leaner module operation the point of minimum hydrocarbon emissions at a 589 K inlet-air temperature when compared to model 1

has been shifted to a higher fuel-air ratio.

Carbon monoxide. - The emission index for the measured carbon monoxide is shown in figure 12. The overall levels shown here are extremely high compared to combustors operating at conventional exit temperatures in the 1300 to 1500 K range. At the highest fuel-air ratios of 0.063 to 0.064 the emission index levels varied from 450 to 650 depending on the combustor inlet-air temperature. Both combustors produced comparable emissions with model 2 showing somewhat lower levels at the combination of lower inlet-air temperatures and high fuel-air ratios. Both combustors exhibited a dramatic increase in CO for fuel-air ratios above 0.040.

At high temperatures an equilibrium condition between the carbon containing species will exist such that a significant portion of the total carbon will be carbon monoxide. Shown for comparison in figure 12 are the levels of carbon monoxide predicted for a theoretical equilibrium composition which were computed using the method of reference 7. These values establish the practical lower limit for carbon monoxide emissions at the combustor exit and are not indicative of inefficient operation. Any calculation of combustion efficiency or combustor exit temperature based on emission measurements must include the effect of the equilibrium carbon monoxide so that combustor performance is not unduly penalized. Additional discussion concerning the treatment of this problem will be found in the subsequent Combustion Efficiency and Average Exhaust Temperature section.

It is possible that the levels of carbon monoxide shown here in the combustor exhaust may not be indicative of the levels found in the exhaust of a gas turbine engine operating at the same conditions. This is because as work is extracted in the turbine expansion process the opportunity exists for equilibrium to be shifted toward lower values of CO by the formation of CO_2. The extent to which this would occur would depend on the actual turbine process and the extent to which reactions were quenched.

Any level of carbon monoxide shown in figure 12 which is greater than the associated equilibrium value indicates inefficient operation. At a given fuel-air ratio, as combustor inlet-air temperature is increased, the measured CO emissions decrease which indicates an increase in combustion efficiency. The efficiency is further increased due to a higher level of equilibrium CO resulting from the higher exhaust gas temperature that accompanies higher combustor inlet temperature at a constant fuel-air ratio.

Oxides of nitrogen. - Measured values of emission index for oxides of nitrogen (NO_x) are shown in figure 13. The most striking feature of the curves is that at a constant inlet-air temperature the maximum NO_x emission index occurs at an intermediate fuel-air ratio. It is possible to explain this phenomena on a qualitative basis. If we begin with the lower fuel-air ratios, as the fuel air-ratio is increased, the reaction zone temperatures are increased and the rate at which NO_x is formed is increased. Eventually a condition is reached where several factors affect this process. As the fuel-air ratio is increased, more of the total oxygen is used in combustion and thus becomes un-

available for NO_x formation. The very large quantities of carbon monoxide formed in the local reaction zones are in competition for the oxygen that is available. In addition, the local fuel air ratio in the vicinity of the modules becomes overly rich, thus reducing reaction zone temperatures and NO_x formation.

The differences between the two combustor models are more evident here than in previous figures. For model 1 the peak in the NO_x emission curves occurs at about a 0.039 fuel-air ratio while for model 2 the peak NO_x occurs at about a 0.045 fuel-air ratio. This result is a consequence of the more open fuel swirler of model 2. Therefore, the depletion of oxygen in the swirler wake (a function of the local fuel-air ratio) would tend to occur at higher overall fuel-air ratios for this design than for model 1. In addition, the peak levels in NO_x achieved with model 2 are higher than with model 1. This may be brought about by a combination of differences between the two models. Recall first that NO_x formation is dependent on the local flame temperature as well as the dwell time at that temperature. For a heterogeneous mixture of fuel and air as is produced by most combustor designs, except for premix types, it is usual to assume that combustion occurs at local equivalence ratios of around 1 even though the overall fuel-air ratio may be varied. As the overall fuel-air ratio is increased the volume of the local flame zone, and hence the dwell time at the maximum temperature, is increased. Therefore, NO_x is increased. For these particular designs which were intended for high temperature operation, and therefore admitted large quantities of air through the fuel swirler, it is possible that local combustion at intermediate overall fuel-air ratios may still be on the lean side of stoichiometric. Therefore, as the fuel-air ratio was increased the local flame temperature was also increased.

Now, when comparing the peak value in NO_x achieved by each of the two combustor designs, it can be seen that the peak occurs at a higher overall fuel-air ratio for model 2 than for model 1. It is logical to expect the NO_x to be higher most likely due to increased residence time but also possibly due to increased local flame temperature as was explained previously. A second factor affecting the difference in the peak NO_x between two combustors is pattern factor. The higher pattern factor of model 2 indicates that more localized high temperature regions exist. This gives a resultant increase in NO_x. This effect of pattern factor has also been noted in reference 8.

Additional information regarding the NO_x formation within the combustor can be obtained by inspection of the NO_x concentration curves shown in figure 14. As expected, the NO_x concentrations for model 2 reached higher levels than for model 1. The curves demonstrate a peak in NO_x production; note, however, that the peak in concentration is displaced to a higher fuel-air ratio than the peak in the emission index. This displacement has no physical meaning but arises as a consequence of the computation of emission index wherein, to a first order, concentration is normalized by the fuel-air ratio. Thus, when the fuel-air ratio increases more rapidly than the concentration, the emission index decreases.

Combustion Efficiency and Average Exhaust Temperature

A widely accepted technique for computing the combustion efficiency from exhaust gas emissions is to determine the amount of unrecovered heat of combustion related to the measured unburned hydrocarbons and carbon monoxide. This technique is commonly employed for combustion systems where the quantity of equilibrium CO is negligible. In these tests the amount of equilibrium CO is significant and therefore some alternate procedure is required. Since combustor exit temperature was the unknown of primary interest, preference was given to a technique which yielded exit temperature directly. The essence of the technique lies in the fact that the composition of the exhaust gas is known. Corresponding to the known inlet temperature, pressure, fuel-air ratio, and composition is a unique equilibrium temperature which can be calculated. This equilibrium temperature may be equal to the ideal equilibrium temperature (if there are no unburned hydrocarbons and the measured CO equals the amount predicted for the ideal composition) or less than the ideal equilibrium temperature (unburned hydrocarbons exist and/or the measured CO contains "inefficient CO" in excess of the ideal equilibrium amount). Details concerning the modification of a standard equilibrium composition program to perform this computation are given in the appendix.

The combustion efficiency, expressed as the ratio of actual to theoretical equilibrium temperature rise, as determined from the exhaust emissions is shown in figure 15. Optimum performance falls in the 0.024 to 0.028 fuel-air ratio range. For higher fuel-air ratios, particularly above 0.040 where CO had been shown to increase rapidly, performance is degraded. At the highest fuel-air ratios the combustor performance was significantly affected by inlet-air temperature. As an example, for model 2 at 0.064 the fuel-air ratio combustion efficiency increased from 91 to 95 percent as inlet-air temperature was increased from 589 to 894 K. Note also, as mentioned in an earlier section, the peak efficiency for model 2 at a 589 K inlet-air temperature was only 99.5 percent.

The combustion efficiency and average exit temperature achieved are shown in figure 16. In order to make differences in performance between the two combustor models more readily apparent, the data for model 1 are repeated as dashed lines in figure 16(b). For the combination of high exit temperature and lower inlet-air. temperatures the combustor model 2 showed an advantage of 1 to 2 percent in combustion efficiency over model 1. At the 839 K inlet-air temperature, however, the combustors gave virtually identical combustion efficiency performance. At an inlet-air temperature of 894 K the combustor model 2 achieved the highest sustained average exit temperature recorded in the test program with a temperature of 2465 K and an efficiency of 95.2 percent.

Smoke Emissions

The smoke number is shown as a function of fuel-air ratio in figure 17 and as a function of combustion exit temperature in figure 18. Smoke data were obtained only for the model 2 combustor. For fuel-air ratios below 0.035 smoke numbers were low. For large engines which would use combustors of this size a maximum smoke number of 25 would meet the Environmental Protection Agency standards (ref. 9). An SAE smoke number of 25 was exceeded at the following combinations of fuel-air ratio and inlet-air temperatures: 0.047 at 589 K, 0.055 at 756 K, and 0.059 at 839 K. A smoke number of 25 was not exceeded at any fuel-air ratio investigated at the 894 K inlet temperature.

The exact mechanism by which smoke is produced in the combustor is not well understood. It is generally believed that large quantities of carbon are formed early in the combustion process and 99 percent or more of this carbon is burned as combustion progresses (ref. 10). By making the initial combustion process richer additional carbon is formed. In these tests therefore as the overall fuel-air ratio is increased the local fuel-rich regions continue to produce more carbon which is not consumed in the combustor. This explains the general trend of the curves in figures 17 and 18. The rate at which carbon is burned is exponentially related to flame temperature. Therefore, increasing the combustor inlet-air temperature should result in decreased smoke for a constant fuel-air ratio. This is in agreement with the observed data trends.

SECTOR TRAVERSE MEASUREMENTS

A limited series of traverses of combustor model 2 were obtained with a single gas sample rake which gave a radially averaged survey of a 120° sector. Typical data obtained from such a survey are shown in figure 19. The combustor inlet-air temperature for this condition was 590 K and the combustor fuel-air ratio was 0.0575.

Although these samples are radially averaged by the probe, surprisingly large gradients still exist in the measured emissions. The local fuel-air ratio shown in figure 19(a) showed variations from -20 to +40 percent of the fuel-air ratio obtained from the metered fuel and airflow. The variations in local CO concentration are less severe than for the other constituents, and the scale for this pollutant has been expanded to dramatize the effects. In previous figures it had been shown that with these combustors at fuel-air ratios below 0.035 that NO_x would rise and fall with local fuel-air ratio. Minimum NO_x concentration in figure 19(b) occurs with minimum local fuel-air ratio which follows the trend mentioned previously. However, the NO_x concentration is not a maximum at the two maximum local peaks in fuel-air ratio. This is because at the high fuel-air ratios the formation of NO_x is suppressed due to the competition with CO for

the diminished supply of free oxygen. Note also that the highest local fuel-air ratio peak is actually in excess of stoichiometric where temperature and NO_x would decrease.

Local combustor exit temperatures were computed using the method outlined in the appendix except that the local rather than the average fuel-air ratios and CO concentrations were used. In general, the local combustor exit temperature varied with the local fuel-air ratio as shown in figure 19(c). Local efficiency tended to vary inversely with local fuel-air ratio (and CO) but minor variations in this trend do exist. For example, virtually identical local fuel-air ratios were measured at the 75° and 108° circumferential positions. However, as the local CO concentration was lower at 108°, the combustion efficiency and local exit temperature (fig. 19(c)) were greater. Given the circumferential temperature distribution shown in figure 19(c), it is possible to compute a kind of pattern factor although not exactly the one defined in the calculations where temperatures defined by a thermocouple measurement were used. In order to be comparable to the pattern factor defined by the thermocouple measurements, the pattern factor based on emissions would have required gas sampling at each radial position rather than a radial average. The pattern factor determined from the exit temperature distribution of figure 19(c) is 0.078. It is reasonable to expect the pattern factor to be small for near-stoichiometric operation as the maximum temperature is restricted to the maximum achievable total temperature. The maximum possible pattern factor for this test point is 0.134.

Since large gradients in the local fuel-air ratio and CO do exist, it is reasonable to question if the technique of using averaged emissions to compute exit temperature correctly accounts for large equilibrium levels of CO that would be present in the local fuel-rich regions. A comparison of the results obtained by using various computational methods (at a combustor inlet temperature of 590 K) is as follows:

Computational technique	Combustor exit temperature, K	Actual temperature rise/theoretical temperature rise, percent
Averaged emissions; emission-based fuel-air ratio, 0.0602	2241	93.6
Incremental emissions	2240	94.8
Averaged emissions; metered fuel-air ratio, 0.0575	2180	92.6

The data used are taken from figure 19. The combustor exit temperature obtained by using averaged emissions or incremental emissions are virtually identical. Note, however, that the efficiencies are not the same due to differences in the theoretical temperature rise as determined from the averaged emissions compared to the average of the

incrementally determined values. This difference arises as a consequence of the nonlinear relation of ideal temperature rise with fuel-air ratio as stoichiometric fuel-air ratio is approached. Also included in table II for comparison is the temperature and efficiency computed by using the fuel-air ratio obtained from the metered fuel and airflow (the method used for the data that was presented earlier in the report).

While it is interesting to compute circumferential variations in combustor exit temperature, approximately 40 times the computer time is required as compared to using averaged emissions. As an example, approximately 400 seconds of computer processing time was required to determine circumferential temperature pattern shown in figure 19(c). Such a large expenditure of computer processing time did not appear justified for more than a few of the sector traverse test points.

Based on the results of the sector traverse measurements, it appears that at high fuel-air ratios, these combustors did not achieve higher combustion efficiency because the CO burnup is mixing limited. To verify that no kinetic limitation on CO burnup are present, computations were performed using the method and kinetic reaction scheme of reference 11. A partial equilibrium combustion was used as an initial step to the kinetic scheme. For equivalence ratios up to 1.0, CO burnup would occur within 4 centimeters of the flameholders if the reactants were perfectly mixed. Kinetic limitations, therefore, appear to be minor compared to mixing limitations.

Combustor Durability

During the course of the test program, the model 1 combustor accumulated approximately 10 hours of the test time and the model 2 combustor accumulated approximately 16 hours of test time at combustor average exit temperatures above 1700 K. The durability of the combustor liners and of the swirl-can modules were of particular concern during the tests. Liner temperatures were monitored for signs of excess metal temperature. For the model 2 design at an inlet-air temperature of 894 K and an average exit temperature of 2465 K, the maximum recorded liner temperature was 1144 K. Examination of the combustors after the tests showed no burning of the module swirlers or flame stabilizers although the model 1 flameholders did exhibit some high-temperature discoloration. No difficulties were encountered here to indicate that stoichiometric operation is not feasible. However, endurance testing was not a part of this program nor was the test pressure level high enough to simulate the more severe conditions associated with higher engine pressure levels.

SUMMARY OF RESULTS

Emissions and performance characteristics were determined for two full-annulus swirl-can combustors operated to near-stoichiometric fuel-air ratios. The measured exhaust gas composition included oxides of nitrogen, carbon monoxide, carbon dioxide, oxygen, unburned hydrocarbons, and smoke. The test conditions included the following: combustor inlet-air temperatures, 589, 756, 839, and 894 K; reference velocities, 24 to 37 meters per second; inlet pressure, 62 newtons per square centimeter; fuel-air ratios, 0.015 to 0.065. The following results were obtained:

1. Combustor average exit temperature and combustor efficiency were calculated from combustor exhaust gas composition as determined from a total traverse at the combustor exit. For fuel-air ratios greater than 0.040, the combustion efficiency decreased with increasing fuel-air ratio in a near-linear manner. Increasing the combustor inlet-air temperature tended to improve combustion efficiency at a given fuel-air ratio. For model 2 at a fuel-air ratio of 0.064 and a combustion inlet-air temperature of 589 K, a combustion efficiency of 91 percent was obtained; this corresponds to an exit temperature of 2250 K. When the combustion inlet-air temperature was increased to 894 K, a combustion efficiency of 95 percent was obtained; this corresponds to an exit temperature of 2465 K. At the lower inlet-air temperature and high fuel-air ratios the combustion efficiency of combustor model 2 was from 1 to 2 percent higher than that of model 1. At 839 K the efficiencies for the two models were virtually identical.

2. The value of fuel-air ratio for maximum NO_x production was dependent on the combustor design and, in particular, the amount of air admitted through the swirl-can module.

3. For fuel-air ratios greater than 0.040, carbon monoxide emissions increased rapidly; at the highest fuel-air ratios the emission index levels were from 450 to 650 grams per kilogram of fuel depending on the combustor inlet-air temperature. The loss in combustion efficiency at high fuel-air ratios was due primarily to carbon monoxide. The oxidation of carbon monoxide in these combustors appears to be mixing, rather than kinetic, limited.

4. Unburned hydrocarbon emissions were below 4 grams per kilogram of fuel even at the highest fuel-air ratios at inlet-air temperatures of 756 K and higher. For an inlet-air temperature of 589 K emissions were 10 grams per kilogram or less.

5. For fuel-air ratios below 0.035 smoke emissions were negligible. An SAE smoke number of 25 was exceeded at the following combinations of fuel-air ratio and inlet-air temperatures: 0.047 at 589 K, 0.055 at 756 K, and 0.059 at 839 K. A smoke number of 25 was not exceeded at any fuel-air ratio investigated at 894 K inlet temperature.

6. No difficulties were encountered with combustor durability at these test conditions to indicate that stoichiometric operation is not feasible.

Lewis Research Center,
National Aeronautics and Space Administration,
Cleveland, Ohio, May 25, 1976,
505-03.

APPENDIX - COMPUTATIONAL INFORMATION

This appendix provides information on the computations associated with the gas analysis. The relations shown here are similar to those of reference 12 although minor differences do exist.

SYMBOLS

A1	correction term for water of combustion removed from sample
A2	correction term for total water removed from sample
COPPM	carbon monoxide concentration in ppm by volume
CO_2PPM	carbon dioxide concentration in ppm by volume
FAR	fuel-air ratio as determined by gas analysis
HCPPM	unburned hydrocarbon concentration in ppm by volume
HCR	atomic hydrogen-carbon ratio (1.92 for jet fuel)
K	correction for water not removed from sample
M_E	molecular weight of combustor exhaust products
M_F	12.01 + (HCR × 1.008)
M_{H_2O}	molecular weight of water
XHUM	water-air ratio (g water/g dry air)

CORRECTION FOR WATER VAPOR REMOVED

The correction assuming total water removal from the carbon monoxide, carbon dioxide, and oxygen samples is given by

$$A2 = A1\left[\frac{200}{200 + XHUM + A1 \times XHUM\left(1 - \frac{COPPM}{10^6}\right)}\right] K$$

where A1 is the correction for water of combustion:

$$A1 = \frac{100}{100 + HCR \times \frac{1}{2}\left(\frac{COPPM}{10^4} + \frac{CO_2PPM}{10^4}\right)}$$

In this experiment the sample was not completely dried but was assumed to have a dew point of 289 K at 17 newtons per square centimeter for which the sample specific humidity is 0.0065 gram per gram air. For this case the value of K is 1.01.

GAS SAMPLE FUEL-AIR RATIO

The gas sample fuel-air ratio is given by

$$FAR = \frac{M_F}{M_E} \times \frac{\frac{COPPM}{10^4} + \frac{CO_2PPM}{10^4} + \frac{HCPPM}{10^4}}{100 - \left[\frac{COPPM}{10^4}\left(\frac{1}{2} + \frac{HCR}{4}\right) + \frac{HCPPM}{10^4} + \frac{CO_2PPM}{10^4}\left(\frac{HCR}{4}\right)\right]}$$

COMBUSTOR EXIT TEMPERATURE

The combustor theoretical equilibrium temperature rise was computed using the equilibrium program described in reference 7. A modified version of this program was also used to compute a temperature rise which corresponded with exit emission measurements. For this purpose the combustion problem was assumed to be a constant-enthalpy, constant-pressure process. A tagged portion of the carbon in the system was allowed to react only to carbon monoxide or elemental carbon, the remainder to react normally; that is, the fuel was structured as

$$X_yC_{1-y}H_{1.9185}$$

where X has been assigned all the properties of carbon but the reaction to XO_2 is not allowed. By increasing the tagged portion of the carbon it was possible to force the equilibrium program to consider a "frozen equilibrium" composition whose carbon monoxide content is greater than would be predicted by equilibrium considerations alone. An iteration was performed until the total carbon monoxide in the system agreed with the experimental measurement. The temperature computed for this composition was assumed to be the combustor exit temperature. Combustion efficiency was then defined as the ratio of this computed temperature rise to the theoretical equilibrium temperature rise.

REFERENCES

1. Niedzwiecki, Richard W.; Juhasz, Albert J.; and Anderson, David N.: Performance of a Swirl-Can Primary Combustor to Outlet Temperatures of 3600° F (2256 K). NASA TM X-52902, 1970.

2. Niedzwiecki, R. W.; and Jones, R. E.: Pollution Measurements of a Swirl-Can Combustor. AIAA Paper 72-1201, Nov.-Dec. 1972.

3. Niedzwiecki, Richard W.; and Jones, Robert E.: Parametric Test Results of a Swirl-Can Combustor. Presented at the Am. Insti. Chem. Engrs. 75th National Meeting, Detroit, Mich., June 4-6, 1973.

4. Adam, Paul W.; and Norris, James W.: Advanced Jet Engine Combustor Test Facility. NASA TN D-6030, 1970.

5. Aircraft Gas Turbine Engine Exhaust Smoke Measurement. Aerospace Recommended Practice 1179, SAE, 1970.

6. Rusnak, J. P.; and Shadowen, J. H.: Development of an Advanced Annular Combustor. (PWA-FR-2832, Pratt & Whitney Aircraft; NAS3-9403) NASA CR-72453, 1969.

7. Gordon, Sanford; and McBride, Bonnie J.: Computer Program for Calculation of Complex Chemical Equilibrium Compositions, Rocket Performance, Incident and Reflected Shocks, and Chapman-Jouquet Detonations. NASA SP-273, 1971.

8. Biaglow, James A.; and Trout, Arthur M.: Effect of Flame Stabilizer Design on Performance and Exhaust Pollutants of a Two-Row 72-Module Swirl-Can Combustor. NASA TM X-3373, 1976.

9. Control of Air Pollution from Aircraft and Aircraft Engines. Federal Register, vol. 38, 1973, pp. 19088-19103.

10. Norgren, Carl T.: Determination of Primary-Zone Smoke Concentrations from Spectral Radiance Measurements in Gas Turbine Combustors. NASA TN D-6410, 1971.

11. Bittker, David A.; and Scullin, Vincent J.: General Chemical Kinetics Computer Program for Static and Flow Reactions, with Application to Combustion and Shock-Tube Kinetics. NASA TN D-6586, 1972.

12. Procedure for the Continuous Sampling and Measurement of Gaseous Emissions from Aircraft Turbine Engines. Aerospace Recommended Practice 1256, SAE, 1971.

TABLE I. - TEST CONDITIONS

[Combustor airflow, 50 kg/sec; combustor inlet pressure, 62 N/cm^2.]

Combustor inlet-air temperature, K	Combustor reference velocity, m/sec
589	25.0
756	31.7
839	35.0
894	37.2

TABLE II. - COMBUSTOR EXIT TEMPERATURE PROFILE FACTORS

Combustor model	Average inlet temperature, T_3, K	Fuel-air ratio	Pattern factor, $\overline{\delta}$	Stator factor, δ_{stator}	Rotor factor, δ_{rotor}
1	580	0.0258	0.44	0.40	0.089
	763	.0200	.27	.23	.050
	844	.0181	.25	.20	.044
	898	.0178	.25	.20	.038
2	605	0.0221	0.53	0.50	0.138
	761	.0221	.47	.44	.121
	845	.0162	.44	.39	.092

TABLE III. - COMBUSTOR EMISSIONS AND PERFORMANCE DATA

[Combustor inlet pressure, 62 N/cm^2.]

(a) Combustor model 1

Combustor inlet total temperature, K	Combustor fuel-air ratio	Ratio of emission based to metered fuel-air ratio	Unburned hydrocarbon		Carbon monoxide		Total oxides of nitrogen		Ratio of calculated temperature rise to theoretical temperature rise, percent	Combustor total pressure loss, percent
			ppm by volume	g CH_2 / kg fuel	ppm by volume	g CO / kg fuel	ppm by volume	g NO_2 / kg fuel		
561	0.0181	1.008	50.6	1.37	285	15.5	58.5	5.2	99.5	3.74
569	.0213	1.005	19.3	.45	170	7.9	76.1	5.8	99.8	3.70
577	.0239	1.003	10.4	.21	132	5.5	94.1	6.4	99.9	3.67
579	.0213	1.004	14.4	.33	149	6.9	81.4	6.2	99.8	3.65
580	.0258	1.001	8.6	.16	150	5.8	104	6.6	99.8	3.79
580	.0280	.999	7.9	.14	210	7.5	120	7.0	99.8	3.82
596	.0261	1.026	5.6	.10	133	5.0	125	7.8	99.9	3.91
594	.0320	.995	6.2	.10	880	27	158	8.1	99.4	4.27
593	.0390	1.000	12.6	.16	3 280	85	196	8.3	98.2	4.28
594	.0441	1.047	59.6	.7	9 474	217	212	8.0	95.4	4.45
594	.0490	1.047	134	1.4	13 174	273	224	7.6	94.4	4.45
594	.0399	1.016	18	.2	4 427	112	183	7.4	97.6	4.39
594	.0398	1.026	17	.2	5 308	134	183	7.6	97.2	4.36
594	.0458	1.041	76	.8	10 293	227	197	7.1	95.3	4.52
595	.0517	1.043	215	2.1	15 842	312	202	6.5	93.7	4.60
594	.0557	1.057	486	4.4	22 718	417	201	6.1	91.7	4.56
594	.0594	1.053	721	6.2	27 264	472	196	5.6	91.2	4.74
594	.0638	1.122	1239	10.0	43 931	713	190	5.1	86.9	4.68
595	.0565	1.065	430	3.9	24 172	438	202	6.0	91.4	4.58
760	0.0154	1.019	0.5	0.02	49	3.2	90	9.4	99.9	5.40
761	.0194	.998	.2	.01	31	1.6	126	10.6	100.0	5.33
760	.0225	1.029	0	0	30	1.3	159	11.5	100.0	5.39
761	.0256	1.025	.1	0	42	1.6	198	12.6	100.0	5.34
761	.0284	1.025	.2	0	90	3.2	236	13.6	99.9	5.31
761	.0306	1.019	.5	.01	154	5.0	271	14.5	99.9	5.11
763	.0200	1.025	1.1	.03	33	1.6	129	10.4	100.0	5.34
764	.0231	1.024	.5	.01	35	1.5	169	11.9	100.0	5.38
763	.0250	1.021	.4	.01	44	1.8	186	12.1	100.0	5.47
762	.0244	1.036	1.0	.02	47	2	172	11.5	100.0	5.31
762	.0282	.976	.9	.02	90	3	220	12.7	99.9	5.39
761	.0322	.978	.9	.01	258	8	263	13.4	99.8	5.44
763	.0365	.976	1	.01	923	25	331	14.9	99.5	5.24
761	.0300	1.054	.3	.01	139	5	227	12.4	99.9	5.22
762	.0361	1.053	.4	0	863	24	324	14.8	99.5	5.37
762	.0398	1.050	.7	.01	2 132	54	371	15.4	98.9	5.42
761	.0441	1.077	2.7	.03	6 767	155	396	14.9	96.9	5.44
761	.0480	1.072	6.3	.1	10 569	224	402	14.0	95.7	5.52
760	.0521	1.073	33	.3	15 416	301	391	12.6	94.5	5.66
759	.0560	1.064	86	.8	21 089	386	364	10.9	93.4	5.61
760	.0601	1.069	213	1.8	28 619	491	365	10.3	92.2	5.73
759	.0638	1.074	390	3.2	34 563	563	351	9.4	92.0	5.76
845	0.0153	1.008	0.3	0.01	34	2.2	114	12.0	99.9	5.74
845	.0181	1.019	.1	0	23	1.3	150	13.4	100.0	5.69
845	.0210	1.023	.4	.01	22	1.0	185	14.3	100.0	5.87
845	.0242	1.027	.6	.01	31	1.3	233	15.7	100.0	5.86
846	.0259	1.025	.7	.01	43	1.7	260	16.3	100.0	5.94
846	.0229	1.032	.7	.02	25	1.1	216	15.4	100.0	5.94
844	.026	1.036	.2	0	55	2	251	15.7	100.0	5.64
843	.032	1.032	.1	0	379	12	386	19.5	99.8	5.80
844	.0381	1.023	.1	0	1 164	31	494	21.4	99.4	5.77
843	.0439	1.020	.1	0	3 781	87	549	20.8	98.5	5.98
843	.0499	1.053	3.8	0	11 791	240	561	18.8	95.8	6.05
843	.0538	1.053	17	.2	15 915	303	556	17.3	95.1	6.09
842	.0576	1.048	43	.4	19 830	354	543	15.9	95.0	6.16
844	.0631	1.035	99	.8	28 845	475	508	13.7	94.5	6.25
845	.0611	1.118	68	.6	31 340	530	501	13.9	92.4	6.07
842	.0522	1.107	7.3	.1	14 659	287	573	18.4	95.1	6.06
840	.0464	1.109	6.7	.1	8 208	179	595	21.3	96.7	5.88
840	.0404	1.073	5.5	.1	1 971	49	543	22.2	99.1	5.76
898	.0157	1.008	.4	.01	22	1.4	146	15.0	100.0	5.91
898	.0178	1.022	.4	.01	19	1.0	170	15.5	100.0	6.05

TABLE III. - Concluded.

(b) Combustor model 2

Combustor inlet total temperature, K	Combustor fuel-air ratio	Ratio of emission based to metered fuel-air ratio	Unburned hydrocarbon		Carbon monoxide		Total oxides of nitrogen		Ratio of calculated temperature rise to theoretical temperature rise, percent	Combustor total pressure loss, percent
			ppm by volume	g CH_2 / kg fuel	ppm by volume	g CO / kg fuel	ppm by volume	g NO_2 / kg fuel		
603	0.0199	0.994	146	3.6	720	35.8	55	4.5	98.8	5.14
605	.0221	.999	92	2.1	466	20.8	71	5.2	99.3	5.24
602	.0239	1.032	75	1.5	438	18.2	86	5.9	99.4	5.20
589	.0221	1.037	169	3.8	768	34	68	5.0	98.9	5.03
594	.0266	1.044	77	1.4	578	22	102	6.2	99.4	4.71
589	.0305	1.028	59	1.0	779	25	126	6.8	99.4	5.37
591	.0342	1.019	41	.6	1 201	35	149	7.2	99.2	5.29
594	.0387	1.009	36	.5	2 231	58	183	7.8	98.8	5.91
590	.0422	1.024	46	.5	5 704	136	215	8.4	97.1	5.27
592	.0460	1.020	78	.9	8 866	195	231	8.3	96.0	5.52
593	.0502	1.014	159	1.6	13 452	272	230	7.6	94.5	5.64
593	.0544	.986	303	2.8	18 201	342	220	6.8	93.3	5.71
593	.0584	.989	590	5.2	24 589	432	208	6.0	91.9	5.86
593	.0621	.984	938	7.8	29 957	498	215	5.9	91.2	5.89
589	.0476	1.034	147	1.6	10 759	229	227	7.9	95.2	5.78
590	.0641	.979	1073	8.6	33 536	542	202	5.4	91.0	5.70
757	0.0221	1.053	6.0	0.1	147	6.6	134	9.8	99.8	6.79
762	.0245	1.053	3.5	.1	128	5.2	171	11.4	99.9	6.62
762	.0270	1.047	2.5	.05	158	5.8	215	13.0	99.9	5.94
763	.0241	1.020	13	.3	123	5	139	9.4	99.9	6.66
758	.0281	1.024	5.3	.1	216	8	191	11.1	99.8	6.89
761	.0320	1.021	3.8	.1	399	12	267	13.7	99.7	7.02
762	.0360	1.024	3.1	0	1 148	32	352	16.1	99.3	6.93
764	.0401	1.021	3.3	0	2 344	59	412	16.9	98.8	7.25
765	.0440	1.019	4.7	.1	3 872	89	487	18.4	98.3	7.14
760	.0480	1.040	11	.1	9 309	197	503	17.5	96.3	7.37
760	.0519	1.033	27	.3	13 599	267	505	16.3	95.2	7.35
761	.0558	1.018	55	.5	19 077	350	481	14.5	94.2	7.27
764	.0599	1.006	102	.9	24 817	427	460	13.0	93.6	7.25
765	.0636	1.000	160	1.3	31 012	506	444	11.9	93.4	7.00
764	.0545	1.020	42	.4	16 585	311	498	15.4	94.7	6.95
763	.0459	1.034	9.9	.1	7 349	162	491	17.8	96.9	6.93
764	.0424	1.033	3.0	0	4 592	109	460	18.0	97.8	6.61
759	.0345	1.022	2.1	0	1 317	38	319	15.2	99.2	6.52
760	.0313	1.011	2.3	0	361	12	258	13.5	99.8	6.17
845	0.0162	1.033	6.5	0.2	123	7.4	98	9.8	99.8	7.41
847	.0182	1.036	3.0	.1	89	4.8	122	10.8	99.9	7.47
844	.0202	1.045	2.2	.05	75	3.7	149	12.0	99.9	7.39
848	.0221	1.048	1.7	0	70	3.1	185	13.6	99.9	7.51
839	.0240	1.053	1.5	0	87	3.6	189	12.8	99.9	7.46
843	.0201	1.004	2.2	.1	74	4	142	11.5	99.9	6.50
844	.0240	1.015	1.5	0	90	4	203	13.7	99.9	6.82
841	.0281	1.013	1.1	0	192	7	277	16.1	99.9	6.95
840	.0321	1.009	.7	0	513	16	357	18.2	99.7	6.99
840	.0359	1.008	.8	0	1 063	30	420	20.6	99.4	7.09
840	.0401	1.053	1.1	0	2 123	53	566	23.3	99.0	7.08
841	.0439	1.043	1.7	0	3 802	88	652	24.7	98.4	7.18
841	.0482	1.079	4.7	0	8 852	186	704	24.4	97.3	7.32
841	.0517	1.059	10	.1	12 677	250	721	23.4	95.8	7.27
837	.0553	1.051	23	.2	16 802	312	681	20.8	95.3	7.60
843	.0452	.998	10	.1	4 356	98	688	25.3	98.3	6.85
843	.0494	1.018	20	.2	10 257	211	716	24.2	96.3	7.19
845	.0561	.993	47	.4	18 702	342	699	21.0	94.9	7.07
843	.0600	.976	120	1.0	23 650	407	658	18.6	94.7	7.25
844	.0640	.966	208	1.7	31 992	520	592	15.8	94.0	7.13
897	0.0479	0.997	12	0.1	7 550	160	845	29.4	97.4	7.41
895	.0538	.982	28	.3	13 501	257	850	26.6	96.4	7.48
897	.0597	.970	73	.6	21 760	376	820	23.3	95.7	7.41
893	.0637	.949	166	1.3	29 578	483	702	18.8	95.2	7.61

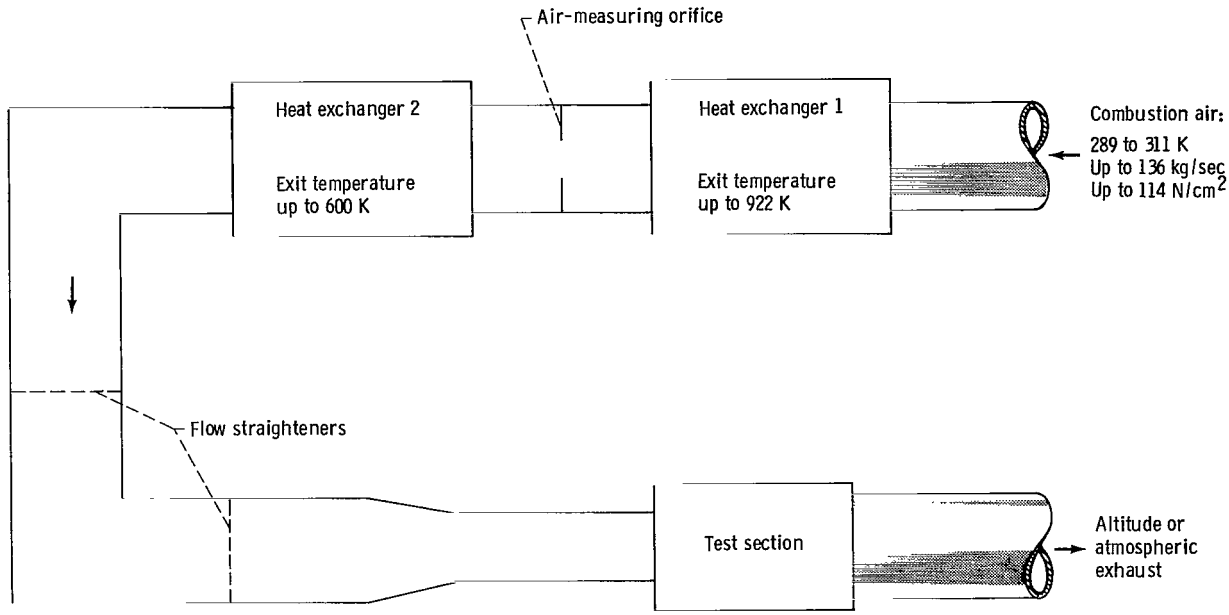

Figure 1. - Schematic of test facility.

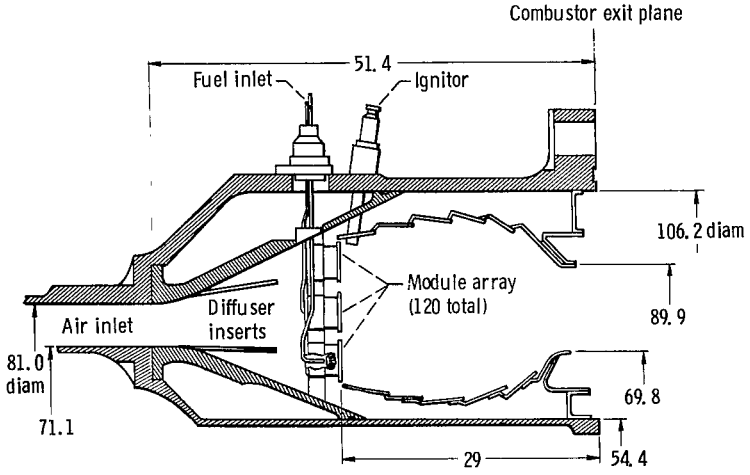

Figure 2. - Annular swirl-can combustor. (Dimensions are in cm.)

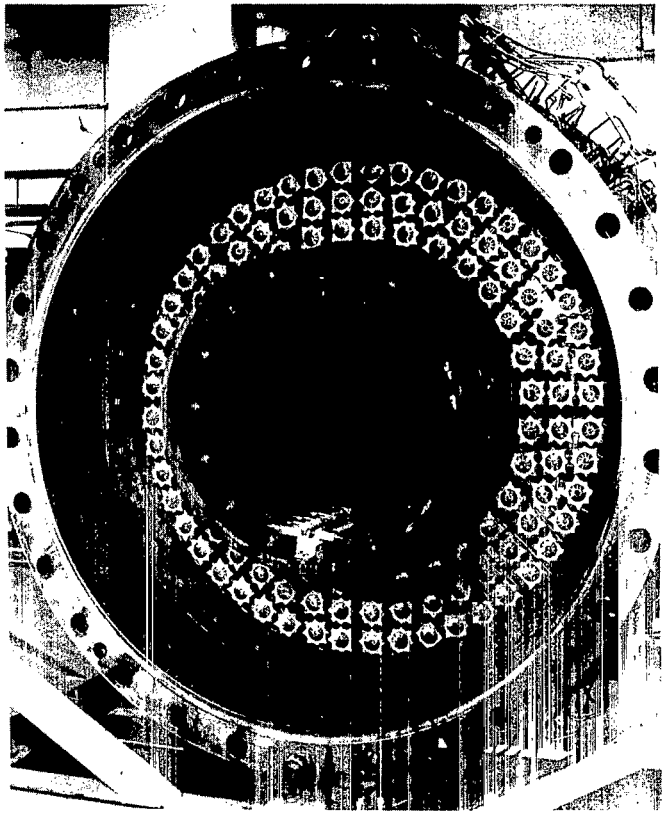

Figure 3. - Typical annular swirl-can combustor. (Inner and outer liners removed to show detail.)

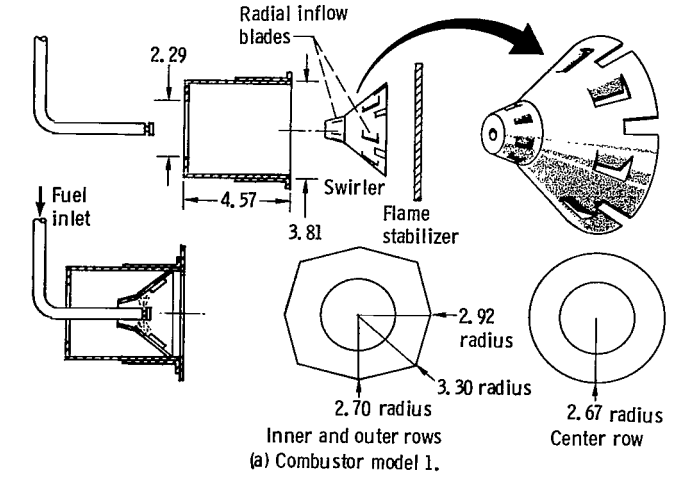

(a) Combustor model 1.

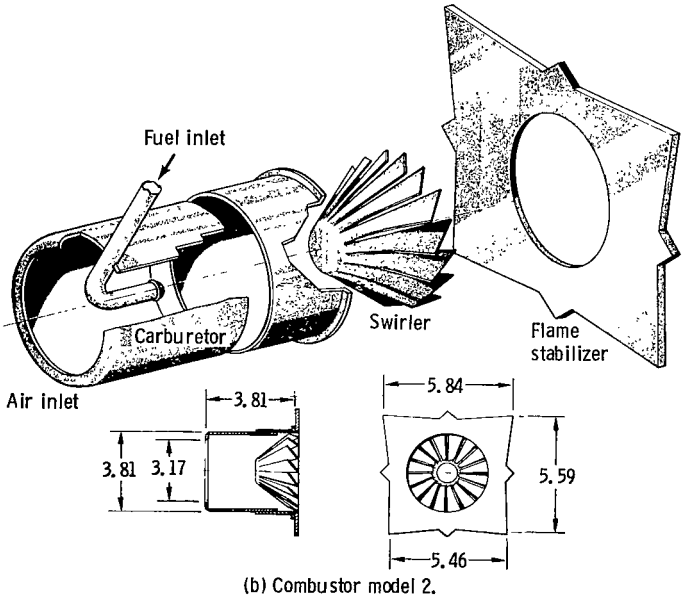

(b) Combustor model 2.

Figure 4. - Swirl-can module details. (Dimensions are in cm.)

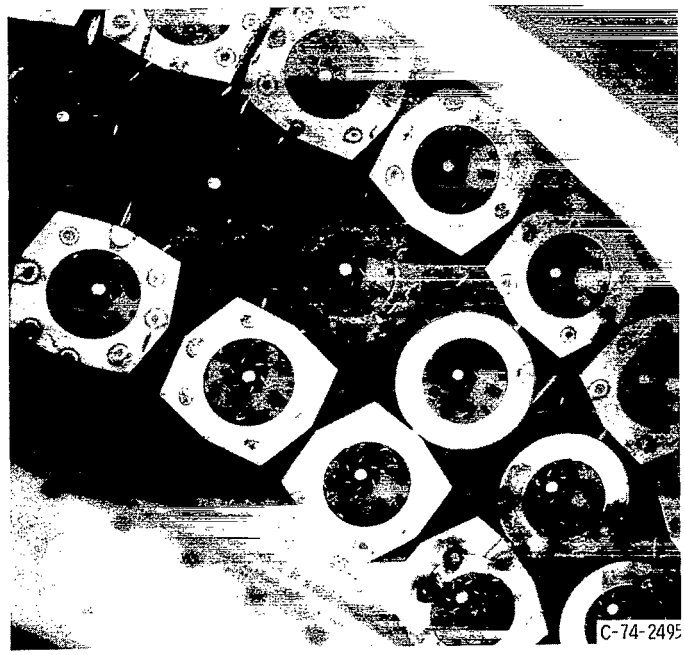

(a) Combustor model 1.

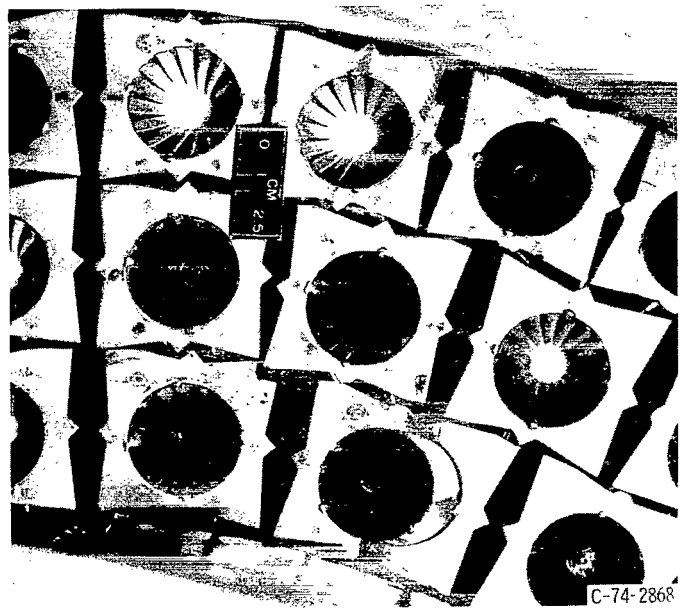

(b) Combustor model 2.

Figure 5. - Sector view of test combustors.

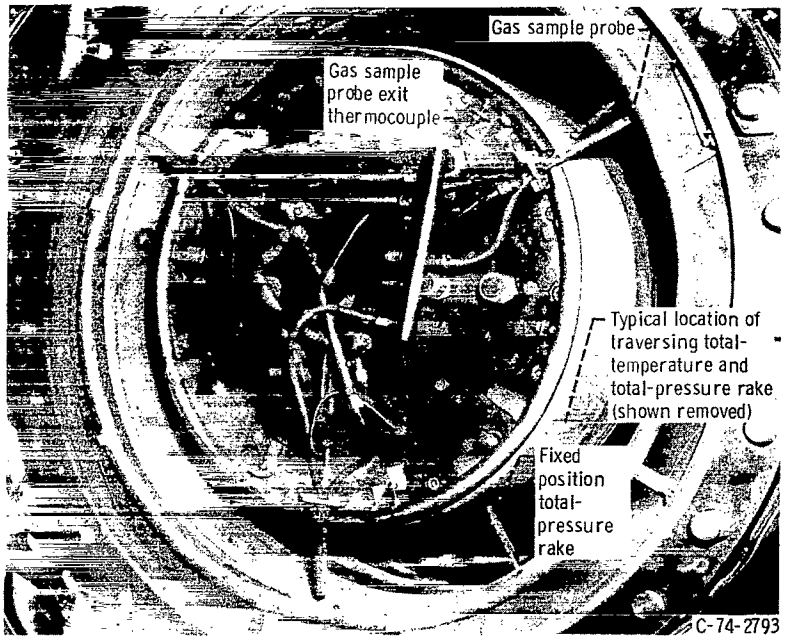

Figure 6. - Probe traverse assembly (view looking downstream).

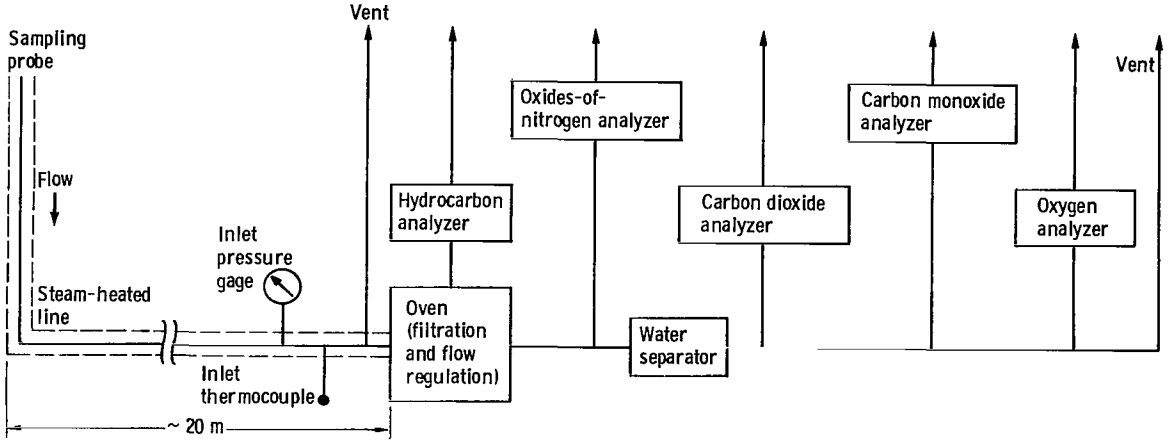

Figure 7. - Schematic of gas analysis system.

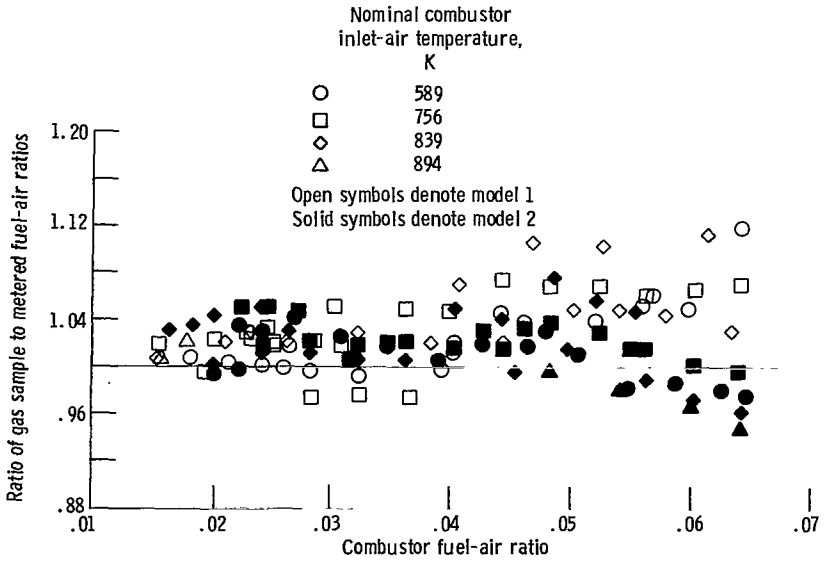

Figure 8. - Gas sample validity check.

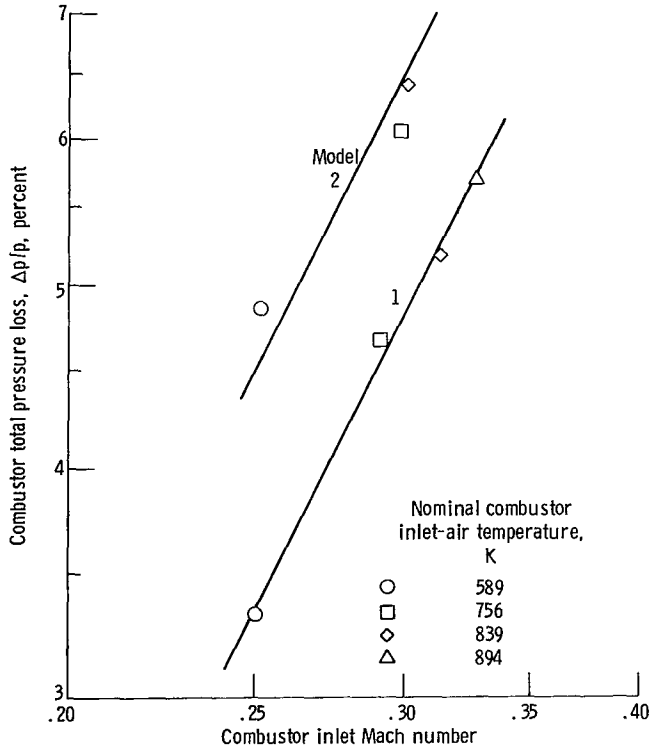

Figure 9. - Combustor isothermal pressure loss.

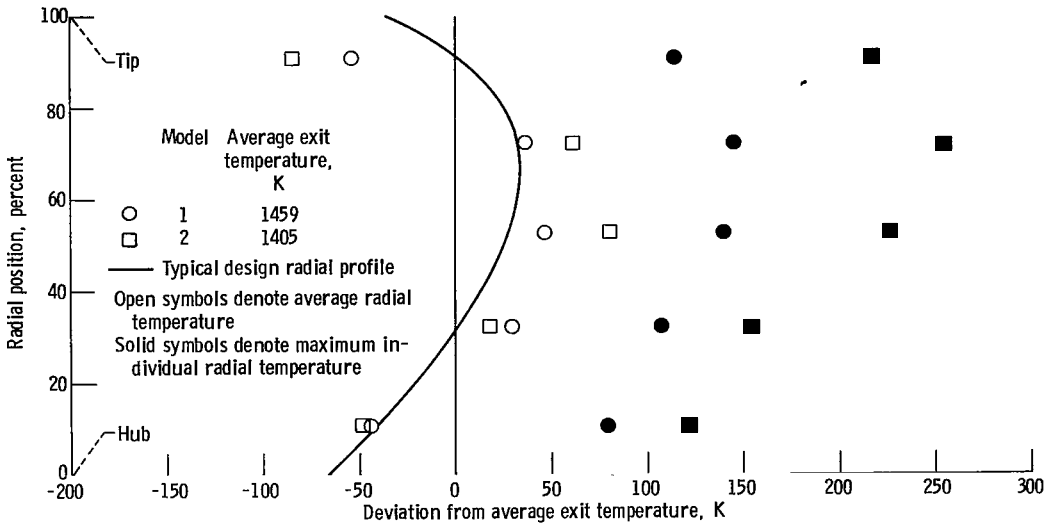

Figure 10. - Typical radial average temperature profiles at the combustor exit. Inlet pressure, 62 meters per square centimeter; inlet temperature, 839 K.

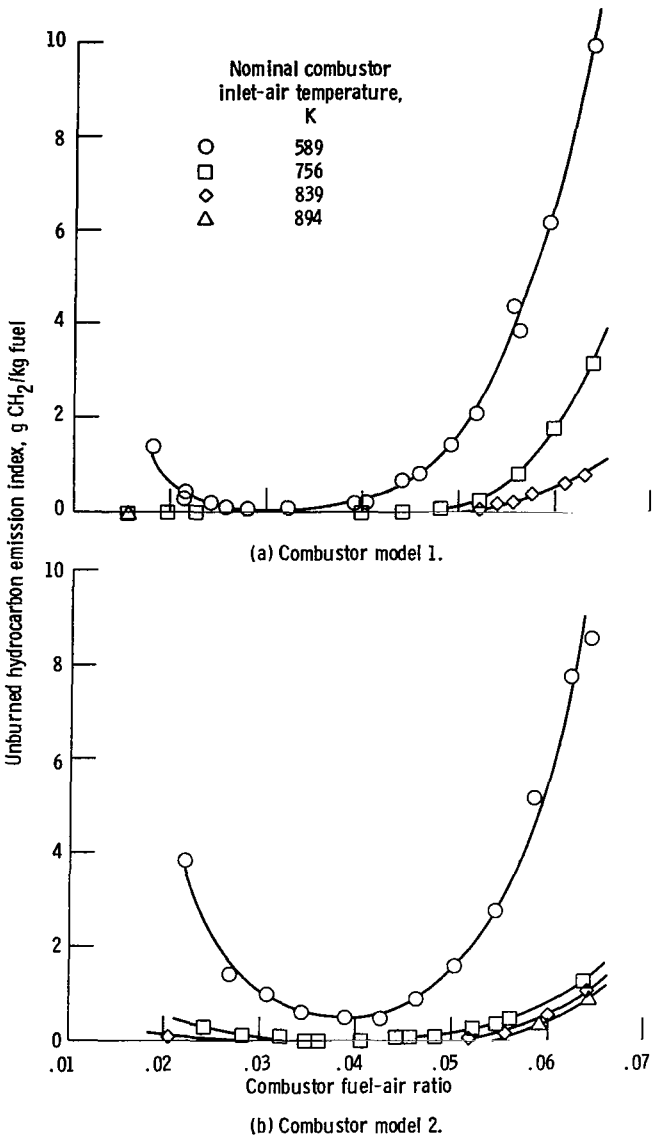

(a) Combustor model 1.

(b) Combustor model 2.

Figure 11. - Unburned hydrocarbon emission index as function of combustor fuel-air ratio. Inlet pressure, 62 newtons per square centimeter.

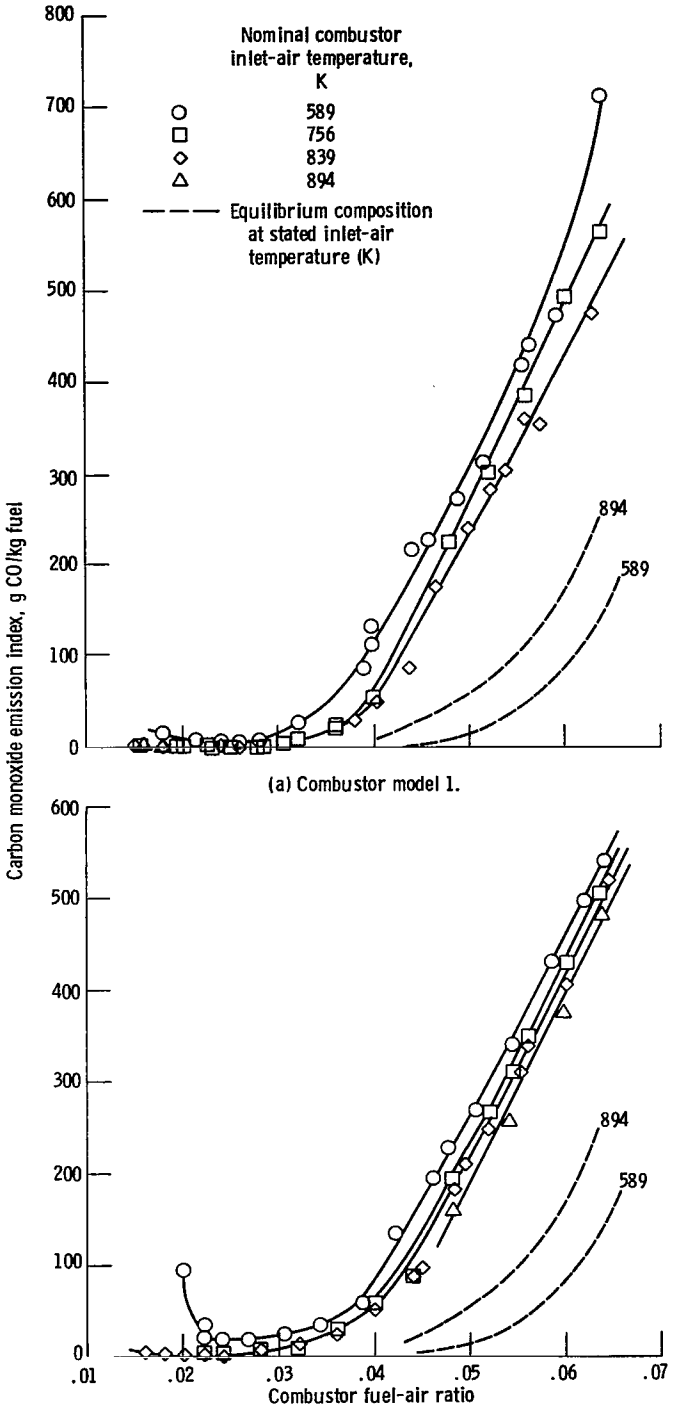

Figure 12. - Carbon monoxide emission index as function of combustor fuel-air ratio. Inlet pressure, 62 newtons per square centimeter.

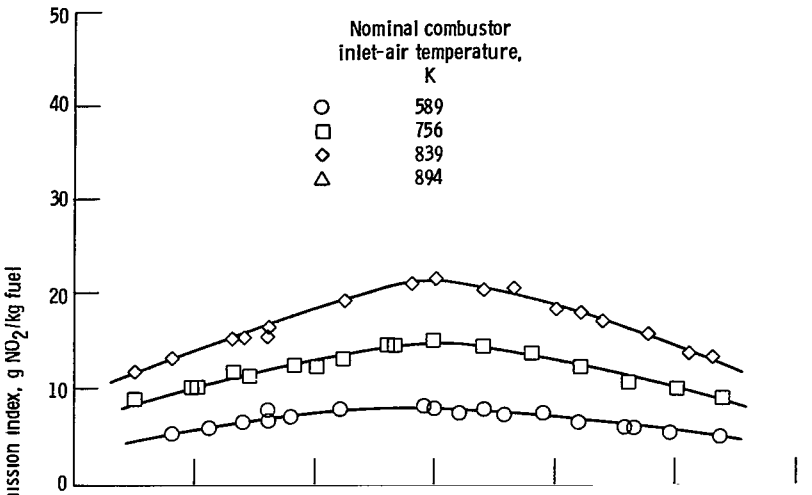

(a) Combustor model 1.

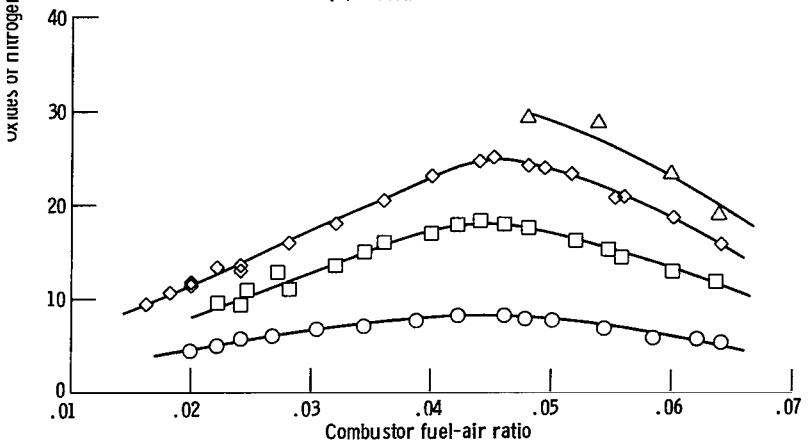

(b) Combustor model 2.

Figure 13. - Oxides of nitrogen emission index as function of combustor fuel-air ratio. Inlet pressure, 62 newtons per square centimeter.

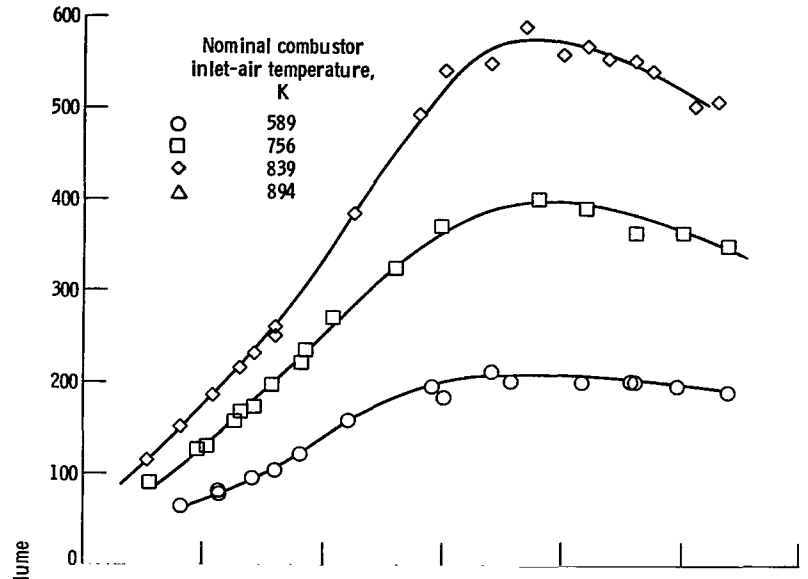

(a) Combustor model 1.

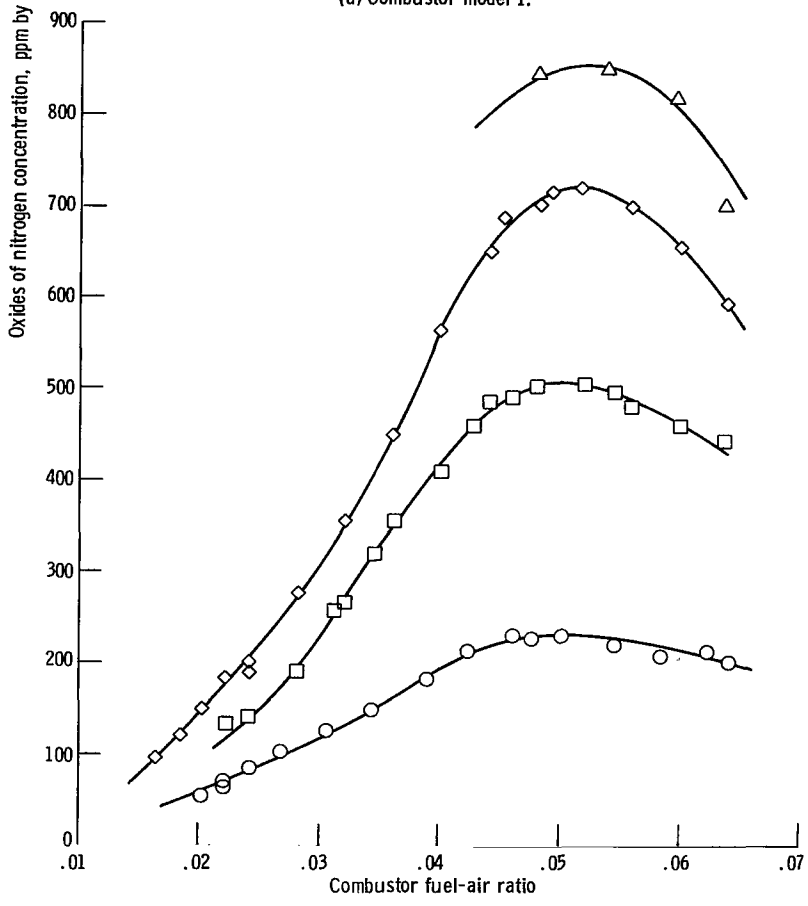

(b) Combustor model 2.

Figure 14. - Oxides of nitrogen concentration as function of combustor fuel-air ratio. Inlet pressure, 62 newtons per square centimeter.

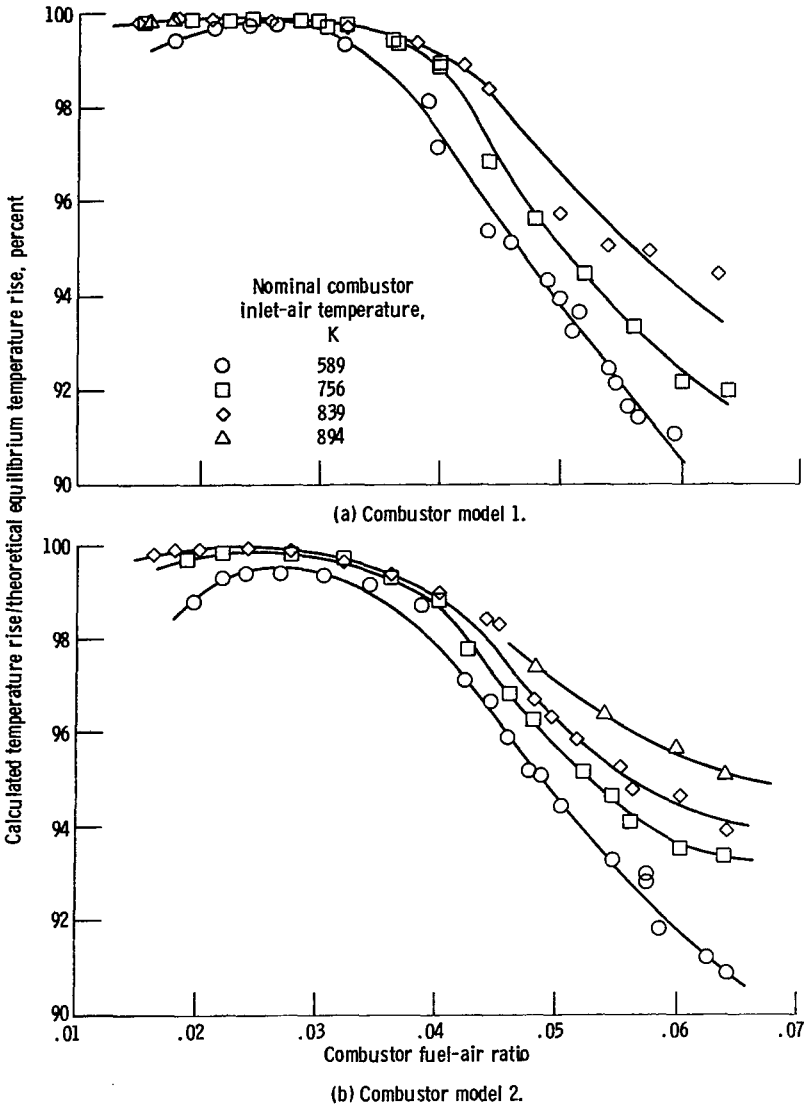

Figure 15. - Combustion efficiency as function of combustor fuel-air ratio. Inlet pressure, 62 newtons per square centimeter.

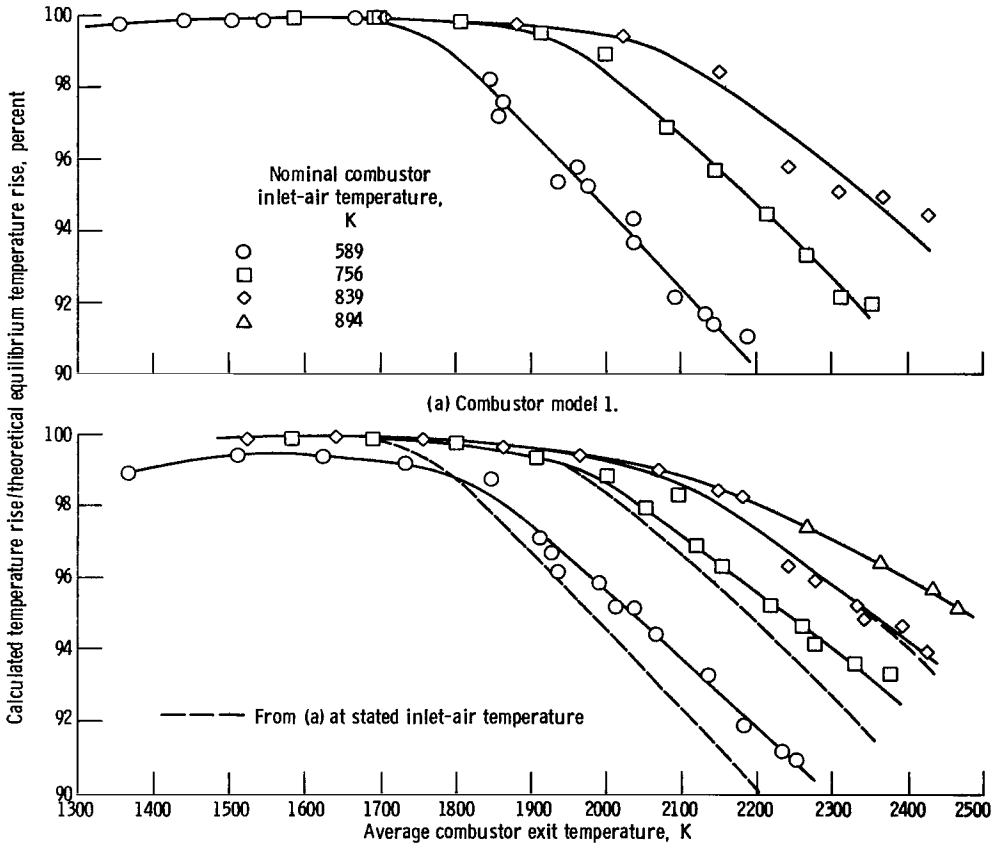

Figure 16. - Combustion efficiency as function of combustor exit temperature. Inlet pressure, 62 newtons per square centimeter.

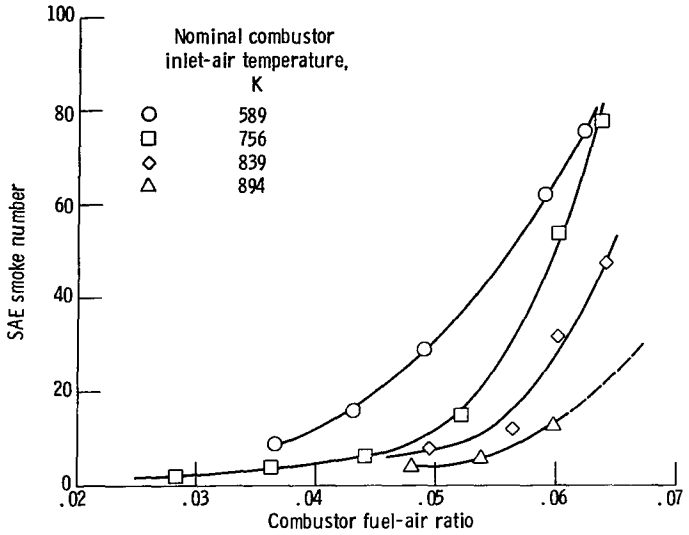

Figure 17. - Model 2 combustor smoke characteristics. Inlet pressure, 62 newtons per square centimeter.

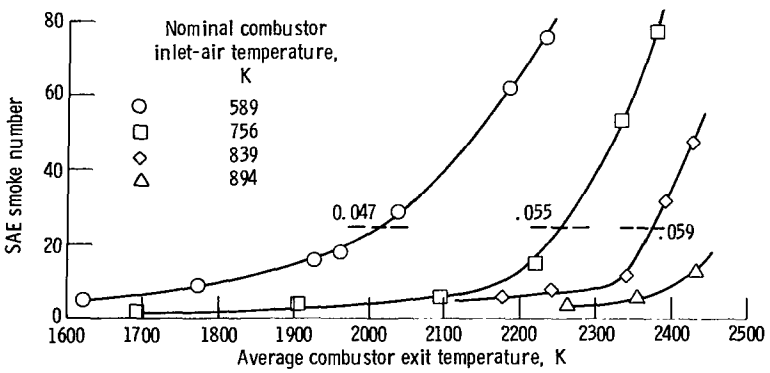

Figure 18. - Model 2 combustor smoke characteristics. Inlet pressure, 62 newtons per square centimeter. Numbers on curves denote fuel-air ratio for smoke number of 25.

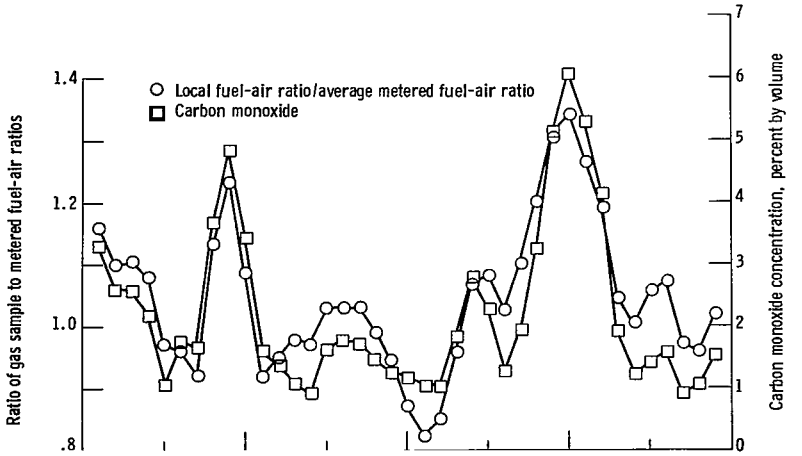

(a) Local fuel-air ratio and carbon monoxide distribution.

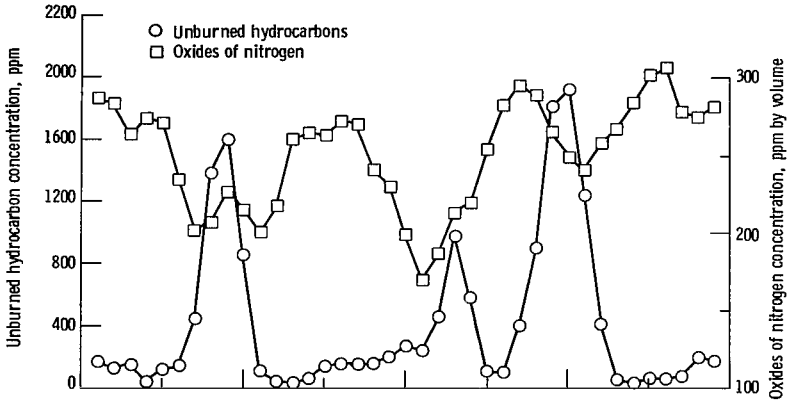

(b) Unburned hydrocarbons and oxides of nitrogen distribution.

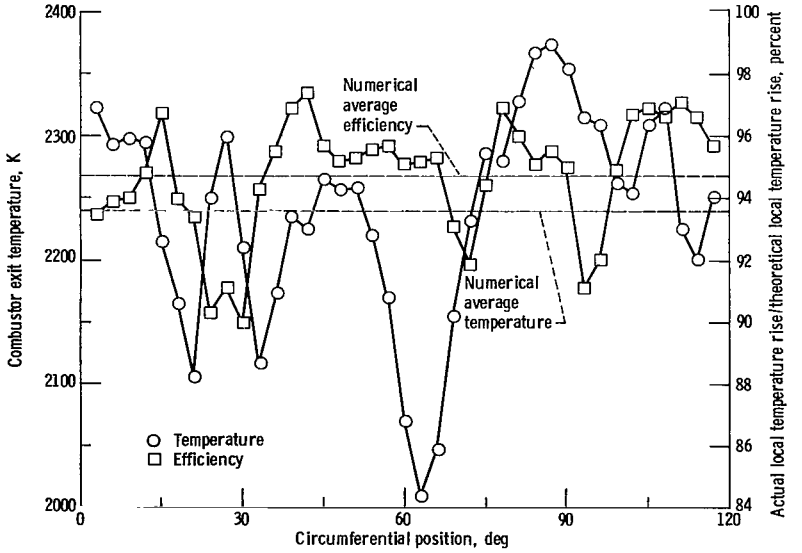

(c) Radial averaged exit temperature and combustion efficiency as determined by gas analysis.

Figure 19. - Typical results obtained from a sector traverse of combustor model 2. Inlet-air temperature, 590 K; inlet pressure, 62 newtons per square centimeter; combustor fuel-air ratio, 0.0575.

"The aeronautical and space activities of the United States shall be conducted so as to contribute . . . to the expansion of human knowledge of phenomena in the atmosphere and space. The Administration shall provide for the widest practicable and appropriate dissemination of information concerning its activities and the results thereof."

—NATIONAL AERONAUTICS AND SPACE ACT OF 1958

NASA SCIENTIFIC AND TECHNICAL PUBLICATIONS

TECHNICAL REPORTS: Scientific and technical information considered important, complete, and a lasting contribution to existing knowledge.

TECHNICAL NOTES: Information less broad in scope but nevertheless of importance as a contribution to existing knowledge.

TECHNICAL MEMORANDUMS: Information receiving limited distribution because of preliminary data, security classification, or other reasons. Also includes conference proceedings with either limited or unlimited distribution.

CONTRACTOR REPORTS: Scientific and technical information generated under a NASA contract or grant and considered an important contribution to existing knowledge.

TECHNICAL TRANSLATIONS: Information published in a foreign language considered to merit NASA distribution in English.

SPECIAL PUBLICATIONS: Information derived from or of value to NASA activities. Publications include final reports of major projects, monographs, data compilations, handbooks, sourcebooks, and special bibliographies.

TECHNOLOGY UTILIZATION PUBLICATIONS: Information on technology used by NASA that may be of particular interest in commercial and other non-aerospace applications. Publications include Tech Briefs, Technology Utilization Reports and Technology Surveys.

Details on the availability of these publications may be obtained from:

SCIENTIFIC AND TECHNICAL INFORMATION OFFICE

NATIONAL AERONAUTICS AND SPACE ADMINISTRATION

Washington, D.C. 20546